



## DYNAMICS OF POST-TENSIONED ROCKING BLOCKS

Clément Barthès<sup>1</sup>, Matías A. Hube<sup>2</sup> and Bozidar Stojadinovic<sup>3</sup>

### ABSTRACT

Dynamic behavior of freestanding slender rigid rocking blocks has been investigated by Makris and Konstantinidis. We extend this study to investigate dynamic response of a slender rigid block that is post-tensioned using an elastic cable placed vertically through its centroid and anchored at its top. First, we derive the dynamic equation of motion for this post-tensioned inverted pendulum system assuming there is no sliding at the contact surface. Then, we investigate its dynamic response to pulse and earthquake excitation and identify the role of block slenderness and post-tension force intensity parameters. Our findings indicated that post-tensioning delays initiation of rocking, increases the ability of the block to resist overturning once rocking initiates, and makes the response of the block less sensitive to motion-to-motion variability. We conclude by investigating the suitability of this dynamic system for use as columns in bridge and building structures.

### Introduction

A rigid block (RB) under rocking motion acts as a non-linear dissipative oscillating system. This fact was recognized by master builders of Ancient Greece, with numerous two-thousand-year old classical columns still standing in evidence of the effectiveness of rocking (and sliding) mechanisms to mitigate the effect of earthquakes on structures. Recent interest in ancient structures brought about analytical evidence on the benefits of rocking (Sinopoli, 1989), (Konstantinidis and Makris, 2005) for classical structures, based on the dynamic analysis of rocking rigid bodies conducted in early 1960's (Housner, 1963).

The fundamental difference between a bending (anchored) single-degree-of-freedom structural (SDOF) system and a free-standing rocking rigid block is in their force-deformation response: a SDOF system hardens while a RB system softens after initiation of rocking (Makris and Konstantinidis, 2003). Therefore, even though rocking is an effective energy dissipation mechanism, the persistent risk of instability and overturning remains and effectively restricts the use of rocking in seismic design.

The goal of this paper is to study the stability of free standing rigid block rocking system

---

<sup>1</sup> PhD Student, Department of Civil and Environmental Engineering, University of California, Berkeley

<sup>2</sup> PhD Candidate, Department of Civil and Environmental Engineering, University of California, Berkeley, Adjunct Professor (on leave), Dept. of Structural & Geotechnical Eng., Pontifica Univ. Católica de Chile

<sup>3</sup> Professor, Corresponding Author, 727 Davis hall, Department of Civil and Environmental Engineering, University of California, Berkeley, CA 94720-1710. E-mail: boza@ce.berkeley.edu

when it is restrained with an unbounded, or partially unbounded, post-tensioning cable. By using different cable configurations, the authors study the possibility of a RB to dissipate energy through rocking without overturning.

### Background

Considering that no sliding occurs between the rigid block and the foundation, a free-standing rigid block is a single degree of freedom system (Figure 1).

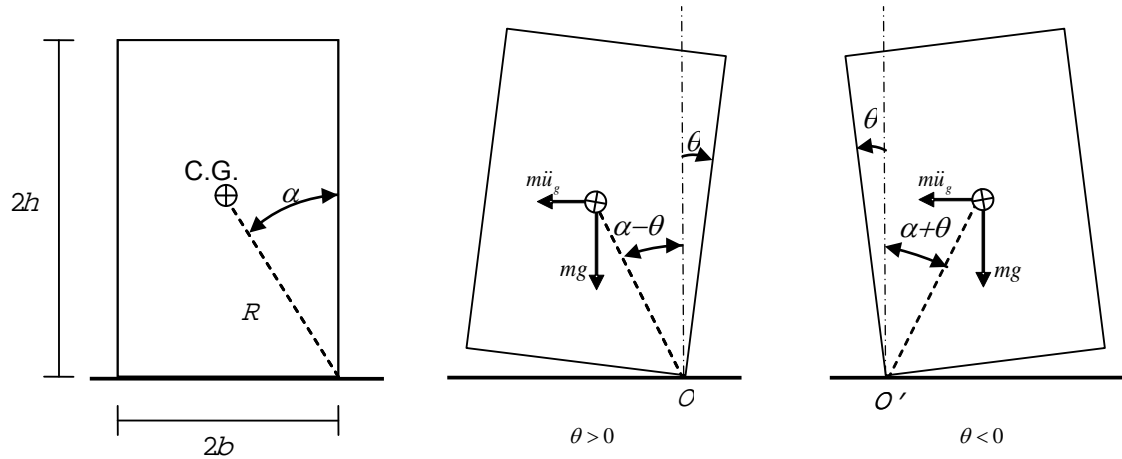


Figure 1. Free standing rigid block oscillator

The equation that describes the free vibration of a RB was first presented by Housner in 1963.

$$I_o \ddot{\theta} = -mgR \sin(\alpha - \theta) \quad (1)$$

where  $\theta(t)$  is the rotation angle,  $I_o$  the moment of inertia respect to the point of rotation,  $m$  the mass,  $R$  the block dimension and  $\alpha$  the slenderness angle, as shown in Fig. 1. The rigid block properties can be expressed by two independent variables. The slenderness angle  $\alpha$ , and a frequency parameter  $p$  defined by by Eq. 2, as follows:

$$p = \sqrt{\frac{mgR}{I_o}} \quad (2)$$

Note that the rocking system is nonlinear and therefore the frequency parameter  $p$  is not equal to a natural frequency of vibration of a linear oscillator. For the case of a rectangular block, the frequency parameter is equal to  $p = \sqrt{3g/4R}$ . To incorporate the energy dissipation at the impact, the rotation is assumed to continue smoothly from point  $O$  to  $O'$  (no sliding) as shown in Fig. 1. The angular momentum during the impact is conserved, therefore the relationship between the angular velocities is obtained (Housner, 1963). Then, the coefficient of restitution  $r$ , relating angular velocities before and after the impact is defined as:

$$r = \left( \frac{\dot{\theta}_2}{\dot{\theta}_1} \right)^2 = \left( 1 - \frac{3}{2} \sin^2(\alpha) \right)^2 \quad (3)$$

Eq. 3 implies that a slender RB loses less energy than a squat one: therefore, damping of rocking motion depends of the block slenderness  $\alpha$ . Due to such dissipation mechanism, the vibration period and vibration amplitude of a rocking RB in subsequent cycles decreases. If the RB is subjected to a horizontal acceleration, the required acceleration to initiate rocking is

$$\frac{\ddot{u}_{g \min}}{g} \geq \tan \alpha \quad (4)$$

The block will overturn when  $\theta \geq \alpha$ . The overturning of a RB subjected to constant horizontal acceleration, to single sine pulse and to earthquake type of excitation was studied (Makris and Konstantinidis, 2003). One conclusion is that the scale effect makes the larger blocks (i.e. block with larger  $p$ ) of two geometrical similar blocks more stable than smaller blocks.

Makris and Konstantinidis (2003) focused their attention on comparing rocking of a free-standing RB and vibration of a conventional single-degree-of-freedom oscillator subjected to horizontal ground acceleration. The solution of the equation of motion of a free-standing RB subjected to ground acceleration  $\ddot{u}_g(t)$  is:

$$\ddot{\theta}(t) = -p^2 \left\{ \sin[\alpha \cdot \text{sign}(\theta(t)) - \theta(t)] + \frac{\ddot{u}_g(t)}{g} \cos[\alpha \cdot \text{sign}(\theta(t)) - \theta(t)] \right\} \quad (5)$$

From their study, Makris and Konstantinidis concluded that the SDOF oscillator and the RB are two fundamentally different systems. For example, the free vibration of a RB is characterized by an increase of the frequency and a decrease of amplitude. Contrary, a SDOF oscillator vibrates with constant frequency. Therefore, the response of one of these two systems should not be used to predict the behavior of the other.

### **Dynamics of a Post-tensioned Rigid Block**

A free-standing RB system is post-tensioned using an elastic-only steel cable through the center of the block cross-section, as shown in Figure 2. This cable is not bonded to the block and results in a vertical force that moves with the rigid block. The post-tension force depends on the strain  $\varepsilon$  of the cable and can be computed as  $P(\theta) = P_0 + k\varepsilon(\theta)$ . Where  $P_0$  is the initial post-tension force (at  $\theta = 0$ ) and  $k$  the elastic cable axial stiffness. The rotation between the axis of the block and the axis of the cable is considered negligible; consequently the post-tension force is modeled as a follower force.

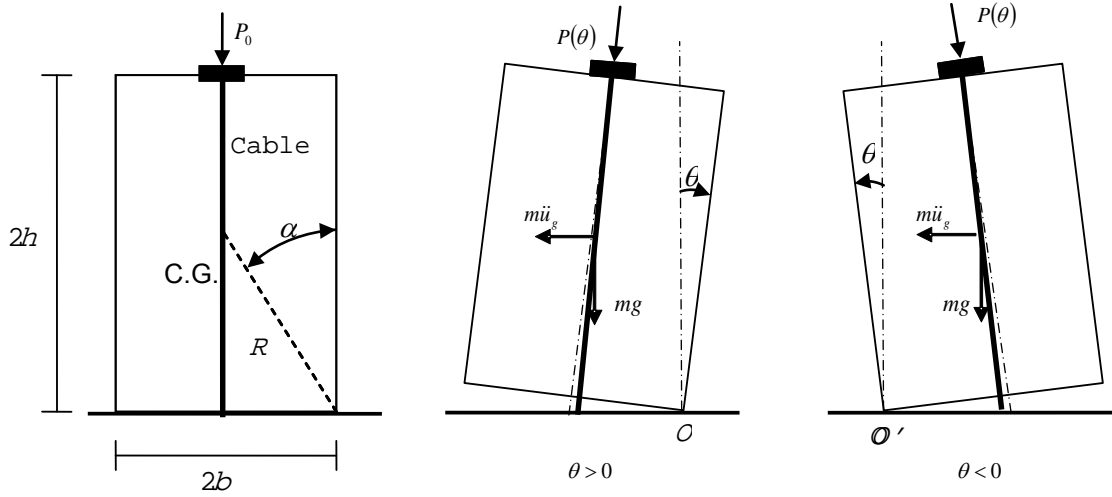


Figure 2. Post-tensioned rigid block oscillator

From Fig. 2, the strain in the cable can be computed as:

$$\varepsilon(\theta) = \frac{\left[4h^2 + 2b^2 - 2b(b \cos \theta - 2h \sin |\theta|)\right]^{1/2} - 2h}{2h} \quad (6)$$

Using Taylor expansion, the strain can be linearized using its first term, as follows:

$$\varepsilon(\theta) \approx \frac{\tan \alpha}{2} \theta + o\left(\theta^{3/2}\right) \quad (7)$$

The strain in the cable for a given rotation depends only of the slenderness of the block. This strain may far exceeds the high strength steel yielding capacity when the RB undergoes large rotations, especially when  $\alpha$  is large (Fig. 3). Therefore the model presented here applies for relatively slender structures post-tensioned using high-strength steel cables.

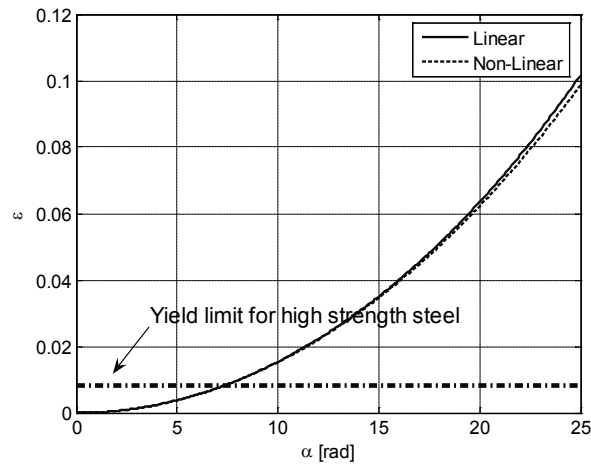


Figure 3. Relative strain of the post-tensioning cable for  $\theta = \alpha$

Fig. 3 also shows that the linearized expression for strain can be used, especially for slender blocks. The cable force can then be represented by two dimensionless parameters as follows:

$$P(\theta) = mg \left( \eta_o + (\eta_\alpha - \eta_o) \frac{\theta}{\alpha} \right) \quad (8)$$

where  $\eta_o$  represents the initial post-tension force at  $\theta = 0$  (divided by the weight), and  $\eta_\alpha$  represents the post-tension force when the RB reaches angle  $\theta = \alpha$ . To obtain the dynamic equation of motion of a RB with an elastic post-tensioning cable, the balance of moment with respect to points  $O$  and  $O'$  is made, leading to the following equations:

$$I_o \ddot{\theta} = -P(\theta)R \sin(\alpha) - m \ddot{u}_g R \cos(\alpha - \theta) - mgR \sin(\alpha - \theta) \quad \text{for } \theta > 0 \quad (9)$$

$$I_o \ddot{\theta} = P(\theta)R \sin(\alpha) - m \ddot{u}_g R \cos(\alpha - \theta) + mgR \sin(\alpha - \theta) \quad \text{for } \theta < 0 \quad (10)$$

Combining Eq. 2, Eq. 8, Eq. 9 and Eq. 10 the solution of the equation of motion of a RB with an elastic post-tensioning cable is:

$$\ddot{\theta} = -p^2 \left\{ \sin[\alpha \cdot \text{sign}(\theta) - \theta] + \frac{\ddot{u}_g(t)}{g} \cos[\alpha \cdot \text{sign}(\theta) - \theta] + \left( \frac{\eta_\alpha - \eta_o}{\alpha} |\theta| + \eta_o \right) \sin \alpha \cdot \text{sign}(\theta) \right\} \quad (11)$$

If the cable is soft enough so that the increase of the post-tensioning force due to block rotation can be neglected (ie.  $\eta_\alpha = \eta_o$ ), Eq. 11 becomes:

$$\ddot{\theta} = -p^2 \left\{ \sin[\alpha \cdot \text{sign}(\theta) - \theta] + \frac{\ddot{u}_g(t)}{g} \cos[\alpha \cdot \text{sign}(\theta) - \theta] + \eta_o \sin \alpha \cdot \text{sign}(\theta) \right\} \quad (12)$$

Energy dissipation is incorporated at each impact using the conservation of angular momentum suggested by Housner, given by Eq. 3. The post-tension cable is assumed remain elastic and, thus, does not dissipate energy. In order to initiate rocking, the normalized ground acceleration has to be large enough:

$$\frac{\ddot{u}_{g \min}}{g} \geq (1 + \eta_o) \tan \alpha \quad (13)$$

The restoring moment versus the rotation angle of a RB with a soft cable for different post-tension values  $\eta_o$  is shown in Fig. 4. It is observed that the restoring moment has a negative (softening) slope. The post-tensioning force moves the force-deformation curve up, making the restoring moment positive for  $\theta > \alpha$ . Therefore, the post-tensioned RB is still unstable but it will overturn at a larger rotation than the corresponding free-standing RB. If the flexibility of the cable is included (i.e.  $\eta_\alpha \neq \eta_o$ ), the stiffness of the system increases and could become positive, as shown in Fig. 4. For  $\eta_\alpha \geq 1 + \eta_o$  the system becomes stable. The dissipation of the system

comes only from the balance of angular momentum, thus the dissipation factor  $r$  from Eq. 3 remains the same. Therefore, post-tensioning can be used to obtain a stable dissipative system.

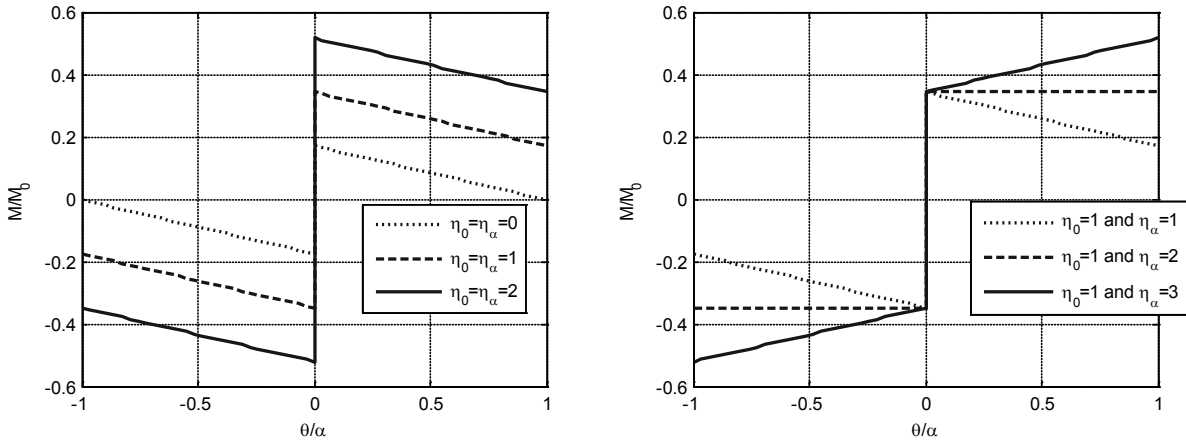


Figure 4. Restoring moment versus rotation ( $M_0 = mg \cdot R$ )

### Dynamic Response

Response of a post-tensioned RB to different types of excitation is shown in this section. The response is calculated by numerical integration of Eq. 11, expressed in state-space as a 2-DOF first order ODE, using a fourth order explicit Runge-Kutta method (Dormand-Prince pair). The system becomes stiff when  $\theta$  becomes very large (beyond overturning angle), therefore an implicit scheme is more efficient to detect overturning.

#### Free Vibration

Fig. 5 shows the free vibration responses of a free-standing and a post-tensioned RB initiated by displacing the blocks by to an angle  $\theta_0 = \alpha/2$ . It is observed that the oscillation period decreases as the rotation angle decreases. The post-tension cable does not add any damping in this formulation, but since the post-tensioned RB oscillates faster than the free-standing RB, the amplitude of rotation decreases faster. Otherwise, the behavior of RBs is very similar. Since no overturning will occur for the given initial conditions, both RBs remain stable.

#### Cosine Pulse Excitation

In order to study the stability of a post-tensioned RB, the response to a ground acceleration pulse (Zhang, 2001) is investigated in this study. The excitation consists of half a cosine ground acceleration pulse with a period of 1sec and amplitude of .7g. While the free-standing RB (without post-tensioning) overturns, the post-tensioned RB remains stable and dissipates the input energy by oscillating as predicted by Eq. 3.

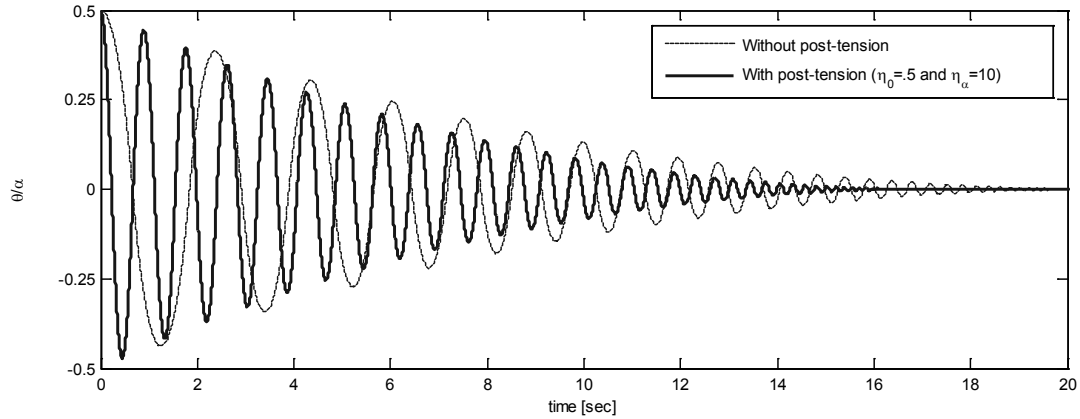


Figure 5. Free vibration response with an initial rotation  $\theta_0 = \alpha/2$ . RB properties are  $p = 2.0$  (1/sec),  $\alpha = 10^\circ$

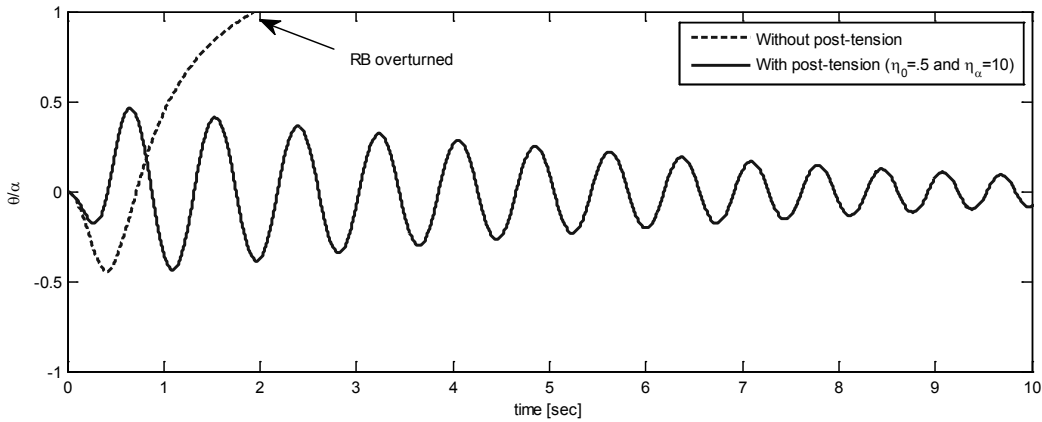


Figure 6. Response to a half-cosine ground acceleration pulse with a period  $T=1$ sec. and an amplitude of  $.7g$  RB properties are  $p = 2.0$  (1/sec),  $\alpha = 10^\circ$

### Practical application

The rocking mechanism can be used as a dissipative system for large bridge structures subjected to earthquake excitation (Chen, 2006). However, the rocking mechanism is rarely used because it is nonlinear and exhibits chaotic behavior, making it difficult to design against instability. The use of post-tensioning cables allows for better control the stability of a rocking structure. It is also affords a great opportunity to use a segmental construction. Prefabricated segments, connected by post-tensioning cables among other means, are now widely used in bridge construction, but their application has been limited in seismic areas due to the complexity of segment joints required to insure adequate earthquake resistance. This limitation stems from engineers' intent to design a joint that does not open during an earthquake. However, opening of such joints caused by rocking may be beneficial.

In the example shown below, the PEER testbed bridge (Ketchum *et al.* 2004) is redesigned such that the columns are made using two segments post-tensioned together using a cable. The joints between the first segment and the foundation, the joint between segments and the joint between the top segment and the cap beam are simply grouted joints traversed only by a centrally-located post-tensioning cable. These joints are, therefore, expected to open and allow for rocking during an earthquake.

The column segments are considered to behave as rigid blocks and the bridge girder is modeled as a lumped mass equal to the mass of the two adjacent mid-spans. The foundation is, also, considered as rigid. The bending and torsional stiffness of the girder is neglected, so the bridge column can be modeled as a post-tensioned RB system. In this study, rocking is allowed only at the joint between the foundation and the foot of the column. For 100' bridge span on both sides of the column, the properties of this post-tensioned RB system are  $p = 1.1225$  and  $\alpha = 4^\circ$ . Note that the lumped mass of the bridge deck on top of the column increases the column RB slenderness to  $\alpha_{column} = 7.1^\circ$ .

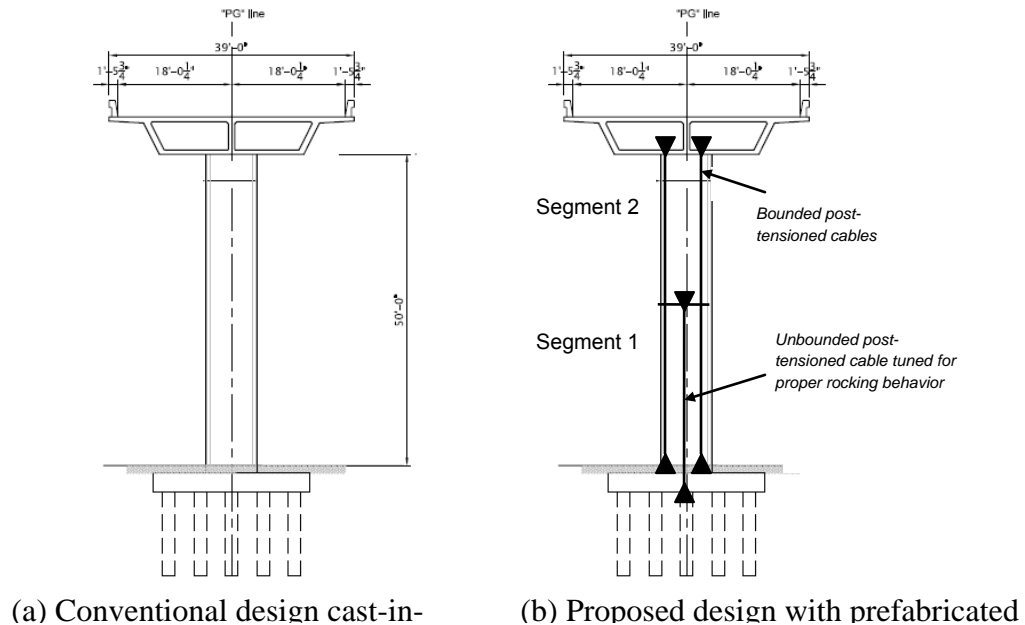


Figure 7. Typical single column bridge section designed by the Californian DOT (CalTrans)

Two design parameters can be used to obtain a stable rocking response of the column. The post-tension force parameters  $\eta_\alpha$  and  $\eta_0$  can be adjusted as needed. Alternatively, the foot of the column at the rocking surface can be widened to increase slenderness  $\alpha$ . Only the first design option is considered in this study. The response to Tabas earthquake (Iran, 1978) is studied.

Without post-tensioning the column will start rocking when  $\ddot{u}_g \geq 0.07g$  and will then overturn. In this study, the post-tensioning force was selected such that rocking of the post-tensioned bridge column initiates when  $\ddot{u}_g \geq 0.2g$ ; this is the principal design parameter in the design procedure for post-tensioned rocking systems. Using Eq. 13,  $\eta_0 = 1.86$ . Large rotations



during rocking lead to large cable forces. To avoid large rotations,  $\eta_\alpha$  has to be large; two values  $\eta_\alpha = \eta_0$  and  $\eta_\alpha = 10\eta_0$  were selected in this study to investigate this design consideration.

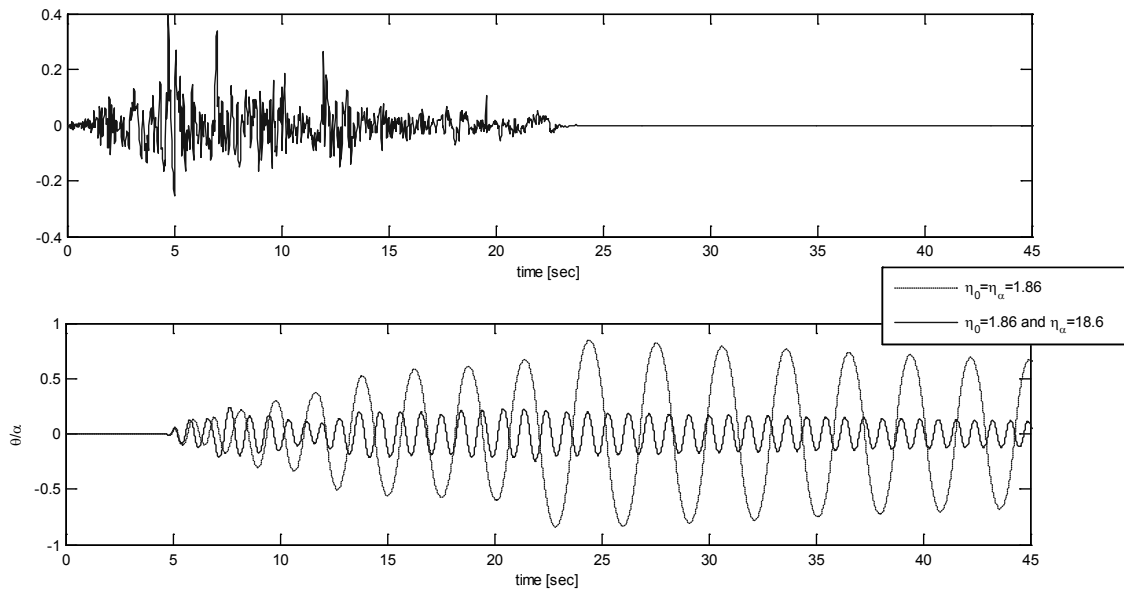


Figure 8. Segmental post-tensioned bridge column subjected to Tabas EQ (a) ground motion; (b) time history of column rotation normalized by column slenderness.

The maximum amplitudes of column rotation are  $\theta_{\max} = 0.85\alpha$  for  $\eta_\alpha = \eta_0$  and  $\theta_{\max} = 0.24\alpha$  for  $\eta_\alpha = 10\eta_0$ . For  $\eta_\alpha = 10\eta_0$  the maximum force is  $F_{pMax} = 5.9 * Weight$ . For the bridge column studied above, a 5in<sup>2</sup> steel cable with a yield stress of 270ksi can be used. This cable should be unbounded along the length of 30ft (Eq. 7 and Eq. 8), corresponding to the length of the first segment of the column (Figure 7). The energy dissipated by the rocking column is small because the structure is very slender (Eq. 3) so an external dissipation mechanism may need to be considered. By increasing the footprint of the column, the dissipation would be larger, but the cable would undergo larger strains which it may not be able to resist. Further research on the post-tensioned rocking bridge column segment solution needs to consider the tradeoffs among these design decisions.

## Conclusions

The rocking behavior of a rigid block post-tensioned to the rocking surface using a linear elastic cable was examined assuming no sliding occurs. It was shown that the post-tensioning of rocking blocks is an efficient way to prevent overturning and thus increase their stability under horizontal excitation. The initial post-tensioning force in the cable will increase the overturning angle of the rigid block as well as the acceleration amplitude that initiates rocking; both of these consequences help stabilize the structure and postpone the event of uplift until larger earthquake magnitudes. In order to obtain a stable structure (with a positive post-uplift stiffness), the tension force in the cable must be allowed to increase with the block rotation. Therefore, the stiffness of the cable plays a major role in system stability. However, under large rotations, the cable may

undergo very large strains, especially for squat structures, so typical cable high strength steels may not be appropriate and other high strength materials with larger ultimate strains may need to be considered. While slender post-tensioned rocking blocks may be optimal from this standpoint, energy dissipation afforded by such systems is small, elongating the time needed for the system to stop rocking. Use of supplemental dampers may be considered in this case, but further understanding of the impact dissipation mechanism when damage is allowed to occur at the impact surfaces, as well as impact wave propagation through the body may also be helpful to fully understand how a rocking system dissipates energy.

### Acknowledgments

This data is based upon work supported by Caltrans project 59A0564: Pre-stressed Structural Systems for Smart California Bridges (PRESS-Bridge): Exploratory Study. This support is gratefully acknowledged. Any opinions, findings, and conclusions or recommendations expressed in this material are those of the authors.

### References

- [1] Chen YH, Liao WH, Lee CL, Wang YP, 2006. Seismic isolation of viaduct piers by means of a rocking mechanism. *Earthquake Engineering and Structural Dynamics*; **35**:713-736.
- [2] FEMA 356, 2000. *Prestandard and Commentary for the Seismic Rehabilitation of Buildings*. Prepared by the American Society of Civil Engineers for the Federal Emergency Management Agency. FEMA, Washington DC.
- [3] Ketchum, M., Chang, V., and Shantz, T., 2004. *Influence of Design Ground Motion Level on Highway Bridge Costs*, Report No. Lifelines 6D01, University of California, Pacific Earthquake Engineering Research Center, Berkeley, California.
- [4] Housner, GW, 1963. The behavior of inverted pendulum structures during earthquakes. *Bulletin of the Seismological Society of America*; **53**(2): 403-417.
- [5] Makris N, Konstantinidis D, 2003. The rocking spectrum and the limitations of practical design methodologies. *Earthquake Engineering and Structural Dynamics*; **32**(6):265-289.
- [6] Konstantinidis D, Makris N., 2005. The rocking spectrum and the limitations of practical design methodologies. *Earthquake Engineering and Structural Dynamics*; **34**:1243-1270.[5] Shenton, H, 1996. Criteria for Initiation of Slide, Rock, and Slide-Rock Rigid-Body Modes. *Journal of Engineering Mechanics* (ASCE); **122**(7):690-693.
- [7] Priestley MJN, Evison RJ, Carr AJ, 1978. Seismic response of structures free to rock on their foundations. *Bulletin of the New Zealand National Society for Earthquake Engineering*; **11**(3), pp 141–150.
- [8] Sinopoli A. 1989. Kinematic approach in the impact problem of rigid bodies. *Applied Mechanics Reviews* (ASME) **42**(11):S233–S244.
- [9] Zhang J, Makris N, 2001. Rocking response of free-standing blocks under cycloidal pulses. *Journal of Engineering Mechanics* (ASCE); **127**(5):473-483.